

Allometric scaling of metabolic rate from molecules and mitochondria to cells and mammals

Geoffrey B. West^{*†‡}, William H. Woodruff^{*§}, and James H. Brown^{†||}

^{*}Los Alamos National Laboratory, Los Alamos, NM 87545; [†]Santa Fe Institute, 1399 Hyde Park Road, Santa Fe, NM 87501; and [‡]Department of Biology, University of New Mexico, Albuquerque, NM 87131

The fact that metabolic rate scales as the three-quarter power of body mass (M) in unicellular, as well as multicellular, organisms suggests that the same principles of biological design operate at multiple levels of organization. We use the framework of a general model of fractal-like distribution networks together with data on energy transformation in mammals to analyze and predict allometric scaling of aerobic metabolism over a remarkable 27 orders of magnitude in mass encompassing four levels of organization: individual organisms, single cells, intact mitochondria, and enzyme molecules. We show that, whereas rates of cellular metabolism *in vivo* scale as $M^{-1/4}$, rates for cells in culture converge to a single predicted value for all mammals regardless of size. Furthermore, a single three-quarter power allometric scaling law characterizes the basal metabolic rates of isolated mammalian cells, mitochondria, and molecules of the respiratory complex; this overlaps with and is indistinguishable from the scaling relationship for unicellular organisms. This observation suggests that aerobic energy transformation at all levels of biological organization is limited by the transport of materials through hierarchical fractal-like networks with the properties specified by the model. We show how the mass of the smallest mammal can be calculated (≈ 1 g), and the observed numbers and densities of mitochondria and respiratory complexes in mammalian cells can be understood. Extending theoretical and empirical analyses of scaling to suborganismal levels potentially has important implications for cellular structure and function as well as for the metabolic basis of aging.

The classic allometric scaling relationship relating metabolic rate (B) to body mass (M),

$$B = B_0 M^{3/4} \quad [1]$$

(with B_0 being a normalization coefficient), was formulated first for mammals and birds by Kleiber in the 1930s (1–4). It has since been extended to a wide range of organisms from the smallest microbes ($\approx 10^{-13}$ g) to the largest vertebrates and plants ($\approx 10^8$ g; refs. 4 and 5). Although the value of B_0 varies among broad taxonomic or functional groups (endotherms, ectotherms, protists, and vascular plants; ref. 4), the value of the scaling exponent (b) is invariably close to $3/4$. Furthermore, many other physiological variables such as lifespan, heart-rate, radius of aorta, respiratory rate, and so on scale with exponents that are typically simple multiples of $1/4$ (2). The origin of the universal quarter power and, in particular, of the $3/4$ exponent in Eq. 1 rather than a linear relationship ($b = 1$) or a simple Euclidean surface-to-volume relationship ($b = 2/3$) has been sought for decades. A quantitative theoretical model (6) has been developed that accounts for quarter-power scaling on the basis of the assumption that metabolic rates are constrained by the rate of resource supply. Accordingly, allometric exponents are determined from generic universal properties of hierarchical transport networks such as the vascular systems of mammals and plants, which occur naturally in biological systems. More generally, it has been shown

that quarter powers reflect the effective four-dimensional fractal-like character of biological networks (7).

In this paper we apply the general ideas underlying the model to show how the scaling of metabolism can be extended down through *all* levels of organization from the intact organism to the cell, mitochondrion, respiratory complex, and ultimately to an individual molecule of cytochrome oxidase, the terminal enzyme of cellular respiration. Accordingly, a relatively simple variant of Eq. 1 connects complex biological phenomena spanning an astounding 27 orders of magnitude in mass from a single molecule to the largest mammal. We know of no precedent for this observation nor any previous theory that could explain it. Its universal character clearly reflects something fundamental about the general principles of biological design and function. The extension of scaling phenomena down to the molecular level offers potentially important insights into the organization of metabolic pathways within cells and organelles as well as into how these fundamental units are integrated functionally at higher levels of organization. In addition to showing how the general principles of the network model account for these phenomena, we show how the turnover rate of the enzyme molecules of the respiratory complex propagates through the hierarchy to limit the maximum aerobic metabolic capacity of whole organisms. Furthermore, the allometric scaling of metabolism at cellular and molecular levels focuses attention on processes associated with aging and mortality.

The origin of $b = 3/4$ for both animals and plants follows from three key properties of their branching transport systems (6): (i) networks are space-filling (thus, for example, they must reach every cell in the organism), (ii) their terminal branch units such as capillaries in the circulatory system or mitochondria within cells are the same size, respectively, for all organisms or cells of the same class, and (iii) natural selection has acted to minimize energy expenditure in the networks. More generally, the universal quarter power can be derived by assuming that the number of terminal units (such as capillaries or mitochondria) in the hierarchical network is maximized when scaled (7). Because this latter argument does not invoke any specific structural design or dynamical mechanism, it can be expected to hold at all levels of biological organization. Because this model works so well for plants and animals with macroscopic vascular systems, it is natural to speculate that similar geometric constraints affect transport processes at the cellular, organelle, and molecular levels. The observation that $b = 3/4$ for unicellular (4) as well as multicellular organisms suggests that the distribution networks within single cells obey the same design principles. Furthermore,

This paper results from the Arthur M. Sackler Colloquium of the National Academy of Sciences, "Self-Organized Complexity in the Physical, Biological, and Social Sciences," held March 23–24, 2001, at the Arnold and Mabel Beckman Center of the National Academies of Science and Engineering in Irvine, CA.

[†]To whom reprint requests should be addressed. E-mail: gbw@lanl.gov.

[§]E-mail: woody@lanl.gov.

^{||}E-mail: jhbrown@unm.edu.

measurements of intracellular transport of metabolic substrates imply the existence of an efficient, organized network (8). Little is known, however, about how characteristics of transport systems constrain rates of metabolic energy transformation at the cellular, organelle, and molecular level. As we shall show, the success of extending allometric scaling models down to the molecular level raises the question of whether there is a real or “virtual” hierarchical transport system inside cells. Complex structures inside cells and mitochondria have been discovered recently that could be components of such a metabolic transport network (9, 10). In any case, the data and their theoretical underpinnings define the problem and suggest that systems that supply cellular metabolism must have fractal-like properties.

We now investigate the interdependence of metabolic processes from the whole organism down to the molecular level. For convenience and because relevant data are readily available, we develop the model in terms of mammals. However, the same principles should apply both qualitatively and quantitatively to all organisms that rely on biochemical reactions and catalysts of the tricarboxylic acid cycle for aerobic metabolism and, in principle, anaerobes as well. It is natural to subdivide an organism into hierarchical levels reflecting pathways of energy flow. At each level the system terminates in a well defined “fundamental” unit. Thus an entire mammal (o) can be viewed as a hierarchy of successively linked networks beginning with a circulatory system that terminates in capillaries. Energy and materials are passed on to cells (c) where other pathways transport them to mitochondria (m) where yet another system transports them to the molecules of the respiratory complex (r) in the inner mitochondrial membranes. These molecules, which are the sites of biochemical aerobic energy transduction, are the final terminal units of the entire metabolic system.

Consider the overall metabolic rate as a function of the masses characterizing the various levels: $B = B(M, M_c, M_m, M_r)$ (the subscript o will generally be suppressed when writing M for the mass of the entire mammal). A mammal is taken to be composed of N_c^o closely packed identical cells, each with metabolic rate $B_c(M, M_c, M_m, M_r)$ such that $N_c^o \approx M/M_c$. Note that B_c , the metabolic rate of an average cell in an intact mammal, depends on the overall body mass, M , and as we now show must be different from its value *in vitro*. From the conservation of energy for flow through the circulatory system that supplies cells we have

$$B(M, M_c, M_m, M_r) = N_c^o B_c(M, M_c, M_m, M_r) \approx \frac{M}{M_c} B_c(M, M_c, M_m, M_r). \quad [2]$$

Combining Eq. 2 with Eq. 1, $B(M, M_c, M_m, M_r) = B_0 M^{3/4}$, gives

$$B_c(M, M_c, M_m, M_r) = \frac{B_0 M_c}{M^{1/4}} \quad [3]$$

such that the metabolic rate of cells *in vivo* decreases with increasing body size as $M^{-1/4}$ (2). Implicit in this derivation is the assumption that capillaries and not cells are the terminal units of the circulatory system such that capillary density varies with body size as $M^{-1/4}$. If cells were the terminal units such that each capillary supplied the same number of cells independent of M , then B_c would be an invariant, and cell or tissue density rather than being independent of M would have to vary with body size as $M^{-1/4}$.

Consider the extrapolation of B from intact mammals down to the cellular level. First recall that B is directly proportional to the overall fluid volume flow rate in the circulatory system. In ref. 6 it was shown how the character of fluid flow changes continuously throughout the network from the aorta to the capillary bed. In the former, pulsatile flow dominates, and little energy is dissipated. However, further down the network, where tubes

narrow, viscosity begins to dominate, leading to the damping of pulse waves such that almost no pulse survives into the capillaries (see *Appendix*). The dominance of pulsatile flow in the overall network plays a crucial role in deriving the three-quarter power law for B , Eq. 1. As the size of a mammal decreases, a point is reached at which even major arteries are too constricted to support pulsatile waves: the system becomes so overdamped that pulse waves can no longer propagate, and a significant amount of energy is dissipated. In this case a calculation of B yields a *linear* (M^1) scaling with mass. The crossover point between this and the $M^{3/4}$ behavior is fairly narrow, and for simplicity we assume that it occurs at a single value of M , which we denote by μ . In reality, the transition is smooth with the precise relationship derivable analytically from ref. 6. Corrections due to this behavior do not affect our conclusions.

We therefore write

$$B(M, M_c, M_m, M_r) = B_0 M^{3/4}, \text{ for } M > \mu \quad [4] \\ = \left(\frac{B_0}{\mu^{1/4}} \right) M, \text{ for } M_c < M < \mu$$

where continuity at $M = \mu$ has been imposed. Eq. 4 leads to the speculation that only mammals with mass greater than μ could have evolved, thereby suggesting a fundamental reason for a minimum size for mammals. By using the model, a calculation (see *Appendix*) predicts μ to be of the order of 1 g, comparable to the mass of a shrew, which is indeed the smallest mammal.

Now, imagine continuously decreasing the overall mass of the organism *below* that of the smallest mammals ($M < \mu \approx 1$ g) until only an isolated cell remains. According to Eq. 4, in this region between the smallest mammal ($M \approx \mu$) and an isolated cell ($M = M_c$) where no real mammals exist, metabolic rate extrapolates *linearly* with M ($B = B_0 M/\mu^{1/4}$) rather than as a three-quarter power law ($B = B_0 M^{3/4}$). The *in vitro* value for the metabolic rate of a mammalian cell is the value of $B_c(M, M_c, M_m, M_r)$ when $M = M_c$, namely $B_c(M_c, M_c, M_m, M_r)$; but this is just the metabolic rate of a cell inside an organism the size of the cell itself and therefore represents a single isolated mammalian cell in tissue culture or a unicellular organism operating at mammalian body temperature. Now, Eq. 2 gives $B(M_c, M_c, M_m, M_r) = B_c(M_c, M_c, M_m, M_r)$, but from Eq. 4 $B(M_c, M_c, M_m, M_r) = B_0 M_c/\mu^{1/4}$, leading to

$$B_c(M_c, M_c, M_m, M_r) = \frac{B_0 M_c}{\mu^{1/4}}. \quad [5]$$

This equation predicts that metabolic rates of single cells isolated from mammals of different body sizes should converge toward a common invariant value, $B_0 M_c/\mu^{1/4}$, rather than preserving the $M^{-1/4}$ scaling, Eq. 3, that they exhibit in the intact organism. Furthermore, this invariant value should approximate the maximum *in vivo* basal metabolic rate when $M = \mu$, the minimum size for real mammals. In other words, the cellular metabolic rate in shrews approximates the maximum possible power output available. Plots of *in vivo* and *in vitro* metabolic rates therefore should intersect at $M = \mu$, where they both have the value given by Eq. 5.

To test these predictions we have plotted data for metabolic rate against mass on a logarithmic scale for 228 mammalian species (11) ranging from a shrew (2.5 g) to an elephant (4×10^6 g) (see Fig. 1). A least-squares fit gives $B_0 = 1.90 (\pm 0.07) \times 10^{-2} \text{ W} \cdot \text{g}^{-3/4}$ and $b = 0.76 \pm 0.01$, which is in good agreement with previous determinations (2–4). Taking $M_c \approx 3 \times 10^{-9}$ g and $\mu \approx 1$ g in Eq. 5, gives $B_c(M_c, M_c, M_m, M_r) \approx 6 \times 10^{-11}$ W for the invariant *in vitro* value of *cellular* metabolic rate. This is in good agreement with the data in Fig. 2, where we have plotted the *in vitro* metabolic rate for cultured cells versus M , the mass of the mammal from which they

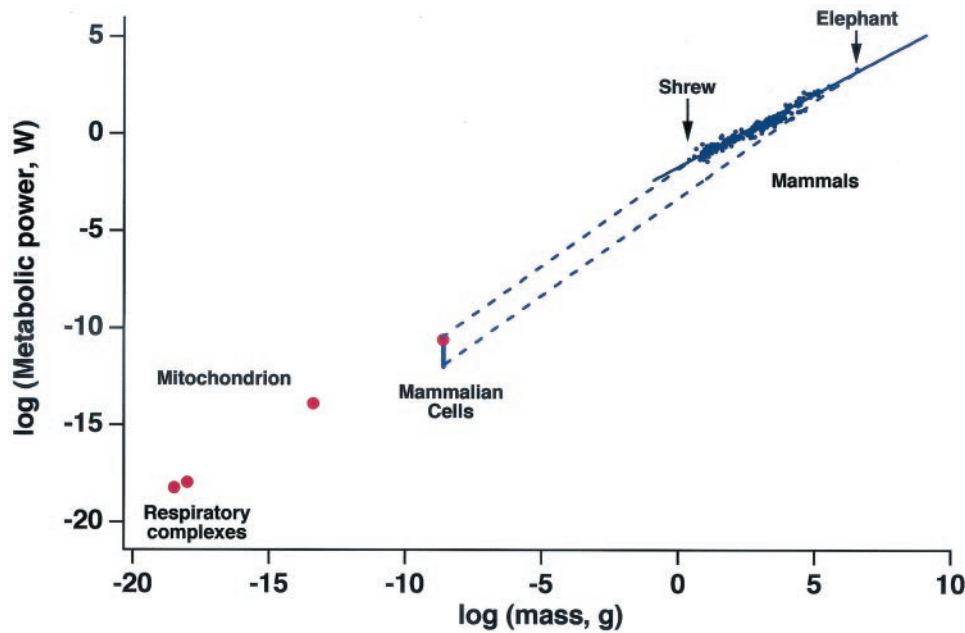


Fig. 1. Basal metabolic rate for mammals as a function of body mass on a logarithmic scale (blue circles). The solid blue line represents the predicted three-quarter power scaling law, covering over six orders of magnitude in mass from a shrew to an elephant. Values for cells *in vivo* for these same mammals are shown as a vertical blue band at a cellular mass of 3×10^{-9} g. These are related to the corresponding whole mammal values by a linear relationship, Eq. 2, as shown by the dashed blue lines. The upper dashed blue line is predicted to intercept the solid blue line at $M = \mu$, close to the mass of a shrew, and to extrapolate to the value for an isolated cell *in vitro* (red data point; see Fig. 2). Also shown (red dots) are *in vivo* values for a mitochondrion, the respiratory complex, and a cytochrome oxidase molecule.

were derived: these data give $B_c \approx 3 \times 10^{-11}$ W, independent of M , as predicted. In Fig. 1 this is entered as a single red point at $M = M_c = 3 \times 10^{-9}$ g and is the same as the value obtained by a linear extrapolation from the smallest mammal down to the isolated cell. Notice also that if whole mammal metabolic rate were naively extrapolated down to the mass of a single cell by using the classic three-quarter power law of Eq. 1, it would give a value of $B_0 M_c^{3/4} \approx 8 \times 10^{-9}$ W. From Eq. 4 this is predicted to exceed the observed value $\approx 3 \times 10^{-11}$ W by a factor of $(\mu/M_c)^{1/4} \approx 135$, which is in satisfactory agreement with Fig. 1. Also shown in Fig. 2 is the variation of the *in vivo* cellular metabolic rate with M ; a power law fit gives good agreement with the exponent of $-1/4$ predicted in Eq. 3. More significantly, it intercepts the invariant *in vitro* line at ≈ 1 g, which is consistent with our theoretical estimate of μ and the mass of the smallest mammal (see Appendix).

Unlike cells, mitochondria and respiratory complexes are terminal units of networks and therefore are required by the model to have invariant properties with respect to the size of the mammal. For example, the power, B_r , generated by the molecules making up the respiratory enzyme complex is governed predominantly by biochemical dynamics, thus it should be invariant not only across all mammals but across all aerobic organisms that rely on the tricarboxylic acid cycle. Actual respiratory turnover rates depend on whether the complex is coupled and transport-limited (*in vivo*) or uncoupled and not supply-limited (*in vitro*), thus the power generated is predicted to be different in the two cases. It is generally accepted that eukaryotes evolved via symbiosis and that mitochondria originally were free-living unicellular organisms. It therefore is reasonable to suppose that mitochondria have metabolic transport pathways similar to aerobic unicellular organisms. Assuming that eukaryotes have evolved hierarchical structures that operate under the general constraints of the network model, we speculate that prokaryotes and mitochondria have self-similar metabolic pathways with fractal-like networks that could be real or virtual and the terminal units of which are respiratory complexes. In that case, their power production (metabolic rates) should scale as $M^{3/4}$. Thus, the

extrapolation of the scaling law down from the isolated cell to mitochondria and the respiratory complex should parallel that of Eq. 1 but scaled down by the factor $(\mu/M_c)^{1/4} \approx 135$:

$$B = B_0 \left(\frac{M_c}{\mu} \right)^{1/4} M^{3/4}. \quad [6]$$

Setting $M = M_m$, Eq. 6 therefore predicts that the metabolic power of a mitochondrion is $B_m = B_0 (M_c/\mu)^{1/4} M_m^{3/4}$; similarly, that of the respiratory complex $B_r = B_0 (M_c/\mu)^{1/4} M_r^{3/4}$. Notice that Eq. 6 agrees with Eq. 5 in predicting the metabolic power of an isolated cell at $M = M_c$. Because the respiratory complex, the ultimate terminal unit of energy production, is universal for aerobes, Eq. 6 also should describe the allometric scaling of metabolic rate for aerobic unicellular organisms. In other words, Eq. 6, which describes the scaling from the respiratory complex up through mitochondria and isolated mammalian cells, should apply also to unicellular organisms. This theory is confirmed by Fig. 3, which shows that metabolic rates of unicellular organisms follow the same three-quarter power scaling relationship as that derived for mammalian cells, mitochondria, and respiratory enzymes.

We also can determine the number of average mitochondria in a typical cell (12, 13); analogous to Eq. 2, the conservation of energy implies $B(M, M_c, M_m, M_r) = N_m^o(M) B_m$. Because terminal units are assumed to be invariant, we have dropped any functional dependence of B_m on $(M \dots M_r)$. Mitochondria are constituents of cells, which in turn are tightly packed constituents of the whole organism, and thus $N_m^o = N_m^c N_c^o \approx (M/M_c) N_m^c$, where N_m^c is the number of mitochondria in a cell. By using Eqs. 1 and 6 we therefore can write

$$N_m^c(M) = \left(\frac{M_c}{M} \right) \left(\frac{B}{B_m} \right) = \left(\frac{M_c}{M_m} \right)^{3/4} \left(\frac{\mu}{M} \right)^{1/4}, \quad [7]$$

showing that the number of mitochondria in the average cell decreases as $M^{-1/4}$, whereas the total number in the whole

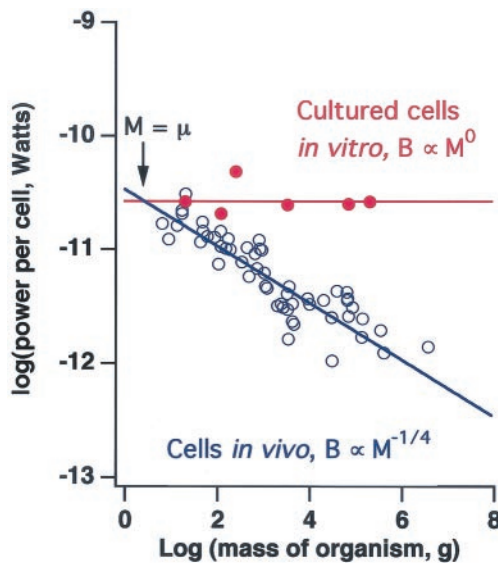


Fig. 2. Metabolic power of single mammalian cells as a function of body mass on a logarithmic scale. Blue circles represent cells *in vivo* calculated for the same mammals as described in Fig. 1. Red circles represent cultured cells *in vitro* of six mammalian species: mouse, hamster, rat, rhesus monkey, human, and pig (32). The solid blue line is the $M^{-1/4}$ prediction for cells *in vivo* from Eq. 3, and the solid red line is the predicted constant for cells *in vitro* from Eq. 5. The two lines are predicted to intersect at $M = \mu \approx 1$ g, at which they have the value $B \approx 3 \times 10^{-11}$ W.

organism should increase as $M^{3/4}$. This relation implies that the average density of mitochondria in the whole organism, $\rho_m^0 = N_m^0/M$, decreases as $M^{-1/4}$, which is in agreement with observation (18). In addition, the ratio of average total mitochondrial volume to whole body volume (assuming a common density) is given by $N_m^0 M_m / M \approx (\mu M_m / M_c M)^{1/4} \approx 0.06 M^{-1/4}$, in agreement with data (M in grams; ref. 19). It is noteworthy that Eq. 7 for the average number of mitochondria in the average cell depends only on the single parameter μ and is independent of B_0 . Taking $M_m \approx 4 \times 10^{-14}$ g gives $N_m^c \approx 300$ for a 50-kg mammal. These are *in vivo* values. Eq. 7 also predicts that after several generations in tissue culture, the number of mitochondria in a cell derived from a mammal of any body size should converge to a single invariant value corresponding to that for $M = \mu$ given by $(M_c/M_m)^{3/4} \approx 5,000$.

Similar reasoning can be extended to the respiratory complex with the result that the average total number in the organism, $N_r^0 = (\mu/M_c)^{1/4} (M/M_r)^{3/4}$, therefore scaling as $M^{3/4}$. The average density in tissue, $\rho_r^0 = N_r^0/M = (\mu/M_c M_r^3 M)^{1/4}$, should decrease similar to that of mitochondria, as $M^{-1/4}$, in agreement with observation (2, 14, 15). Taking $M_r \approx 1 \times 10^{-18}$ g, the number of complexes in an average mitochondrion is predicted to be $N_r^m = (M_m/M_r)^{3/4} \approx 3,000$, independent of M , in accord with the idea that both are invariant units. This argument can be extended in a similar fashion beyond the respiratory complex to the cytochrome oxidase molecule, which is the terminal enzyme of cellular respiration.

To test these ideas we have added three further data points to Fig. 1 (16–19) corresponding to the metabolic power at 37°C of a single mitochondrion, a single molecular unit of the mitochondrial respiratory complex (NADH dehydrogenase plus cytochrome *bc1* plus cytochrome oxidase), and a single molecule of mammalian cytochrome oxidase. The power data for the molecules are calculated by multiplying the free energy of the catalyzed reactions by the *in vivo* turnover rates in intact, resting cells at 37°C [for cytochrome oxidase, reduction of O_2 by cytochrome *c*; for the respiratory complex, reduction of O_2 by

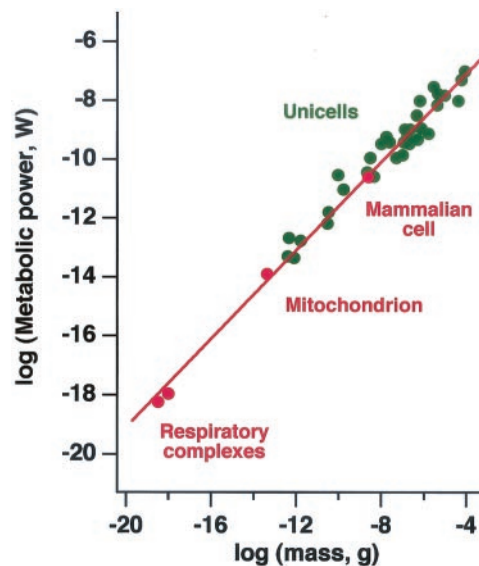


Fig. 3. Metabolic power of an isolated mammalian cell, mitochondrion, respiratory complex, and cytochrome oxidase molecule (red dots) as a function of their mass on a logarithmic scale. The solid red line is the $M^{3/4}$ prediction (Eq. 6). Also shown are data for unicellular organisms (green dots), which, when adjusted to mammalian body temperature, closely follow the same scaling relationship.

NADH (20)]. Nearly all the metabolic power of aerobic organisms is produced by these reactions; the molecular enzyme complexes that catalyze them constitute the irreducible units of cellular respiration or, viewed another way, the ultimate terminal units of the transport network(s) that supply aerobic metabolism. As predicted, the data are well fit by Eq. 6, including both the slope and the normalization constant (Fig. 3).

A summary of our analysis of the scaling of metabolic rate, including both predictions and empirical evaluation, is shown in Fig. 4. The entire plot spans 27 decades of mass and is fitted with just three parameters, B_0 , b , and μ . The latter two, $b \approx 0.75$ and $\mu \approx 1$ g, are determined by the model, leaving only a single free parameter, B_0 , the overall scale of metabolism. Thus, over this entire range, the scaling exponent is very close to $3/4$ except for the region between the smallest mammal and the invariant isolated cell where it is very close to being linear. We know of no previous theory that could predict how the power law obeyed by intact animals can be extrapolated to an isolated cell, a mitochondrion, and an enzyme molecule of the respiratory complex. This argument could be turned around: knowing the scale of power generation at the molecular level is sufficient to predict the metabolic rate of individual mitochondria and cells (whether *in vitro* or *in vivo*) as well as intact mammals.

The data point for the power generated by the respiratory complex shown in Fig. 1 is for a coupled unit *in vivo*. The value for an uncoupled unit, which represents the maximum output of the respiratory complex, is ≈ 300 times larger. This factor propagates through the hierarchy of networks such that ultimately the maximum metabolic output of both a mitochondrion and an isolated cell should be of the order of 300 times larger than their basal rates. Naïve extrapolation to intact mammals would suggest that maximum aerobic capacity also should be ≈ 300 times basal metabolic rate. In fact, this is an absolute limit that is never reached because of limitations on the supply network. For example, flight muscle cells of hovering hummingbirds can indeed metabolize at ≈ 200 times their basal rates (2, 8). However, the coupled circulatory and respiratory systems cannot distribute metabolites and oxygen to all tissues simultaneously at this rate. During maximum activity, supply to non-

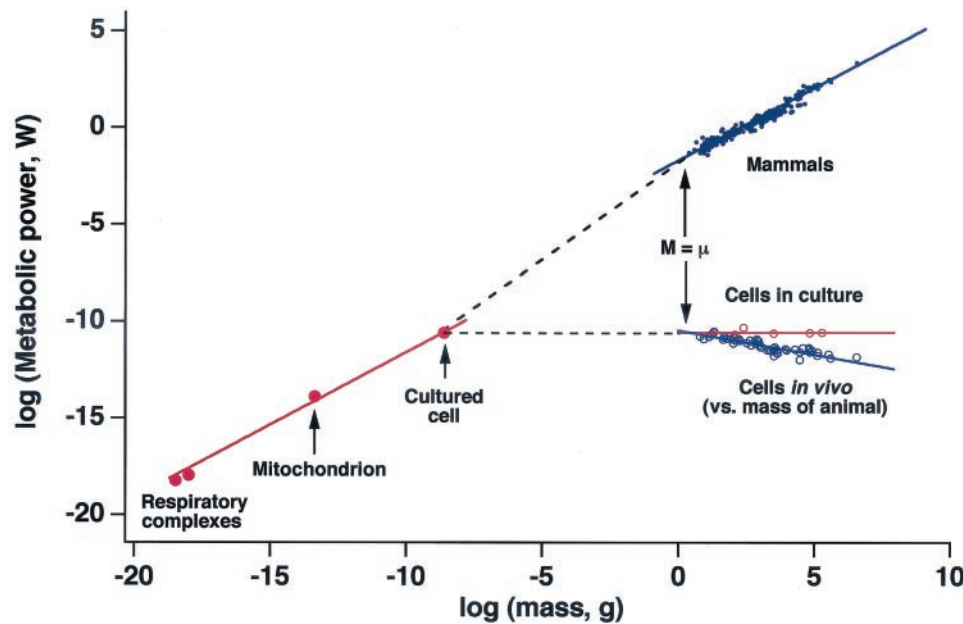


Fig. 4. A logarithmic plot of metabolic power as a function of mass, which summarizes Figs. 1–3. The entire range is shown, covering 27 orders of magnitude from a cytochrome oxidase molecule and respiratory complex through a mitochondrion and a single cell *in vitro* (red dots), up to whole mammals (blue dots). The solid red and blue lines through the corresponding dots are the $M^{3/4}$ predictions. The dashed blue line is the linear extrapolation from $M = \mu$, the approximate mass predicted and observed for the smallest mammal to an isolated mammalian cell, as shown in Eq. 4. The open circles represent the cellular data shown in Fig. 2: red indicates cells *in vitro*, and blue indicates cells *in vivo*.

muscle tissues is reduced and the whole organism aerobic metabolic rate is increased over basal levels by a maximal factor of 10–30, an order of magnitude less than the factor of 300 that would be observed if all respiratory complexes in all mitochondria in all cells could be supplied so as to simultaneously transform energy at maximal rates. The factor of 10–30 is similar to the ratio of maximally stimulated or decoupled cells to that of the metabolic rate of resting cells.

Lifespan (T) also satisfies an allometric scaling law, although the scatter of data are significantly greater than for metabolic rate (2, 21), partly because of the problem of obtaining reliable data. Nevertheless, data for mammals suggest that $T = T_0 M^{1/4}$. As with metabolic rate, the exponent is essentially the same for all taxonomic groups, but the normalization, T_0 , differs. Now, from Eq. 1 the specific metabolic rate $\bar{B} \equiv (B/M)$, the power required to support a unit mass of an organism, scales as $\bar{B} = \bar{B}_0 M^{-1/4}$. This implies the remarkable result that on the average all mammals use approximately the same amount of metabolic energy to support a given unit mass during their lifetimes. This quantity of energy is given approximately by $T\bar{B}/M \approx 4 \times 10^6 \text{ J}\cdot\text{g}^{-1}$, corresponding to roughly 10 mol of O_2 per gram of mass per lifespan (assuming that the average lifetime metabolic rate is 2.5 times the basal value). Another intriguing invariant is the number of heartbeats in a lifetime, $\approx 1.5 \times 10^9$ for mammals. This value follows from the empirical observation (2) that heart rate scales as $M^{-1/4}$, a result predicted by the model for the cardiovascular transport network (6).

Although these invariants have been recognized for some time (2, 21, 22), the possible implications at the molecular level, suggested by Fig. 4, have not. A more fundamental relevant universal invariant quantity is the number of turnovers in a lifetime of the molecular respiratory complexes per cell, which we calculate to be $\approx 1.5 \times 10^{16}$. This observation is consistent with the widely held radical damage hypothesis of aging and mortality (23). Free radicals and other oxidizing compounds are byproducts of respiratory metabolism that may react with vital cellular components, causing cumulative and ultimately lethal damage. It perhaps is noteworthy that pigeons and rats have

approximately the same body mass and metabolic rate yet rats live for up to 4 years, whereas the maximum lifespan of pigeons is almost 40 (23). Perhaps not coincidentally, rat mitochondria produce radicals at a rate 10 times greater than pigeon mitochondria. The invariant O_2 consumption per cell per lifespan that arises from Fig. 4 suggests specific theoretical and experimental studies to test whether production rates of free radicals and other byproducts of metabolism can be a major cause of mortality and the allometric scaling of lifespan.

As already mentioned, there now seems to be general agreement that eukaryotic organisms evolved via symbiosis and that mitochondria and chloroplasts were once free-living prokaryotes. This implies a three-stage evolution of the network that supplies aerobic metabolism of mammals and other multicellular eukaryotes. The aerobic bacteria that were the ancestors of mitochondria possessed networks that shunted metabolites efficiently to the enzymes of the respiratory complex. When unicellular eukaryotes evolved they were able to take advantage of the energy transforming systems of their mitochondrial symbionts. To do so, however, they had to evolve efficient networks to convey materials between cell surfaces and the mitochondria. Finally, the evolution of large, complex multicellular organisms required the evolution of efficient circulatory and respiratory systems to convey metabolic substrates from specialized structures on the body surface to the cells. Interestingly, all these systems seem to exhibit the features of quarter-power allometric scaling predicted by our fractal-like models of biological networks.

In conclusion, we have shown how a theory of allometric scaling integrates power production across all levels of biological organization from the molecules of the respiratory complex, through mitochondria to unicellular organisms and isolated cells in tissue culture, and on up to multicellular organisms. This theory, based on fractal-like distribution networks, can explain variations in metabolic rate over an amazing 27 orders of magnitude. Perhaps one of our most intriguing results is the prediction that the metabolic power of a cultured mammalian cell should be the same, independent of the mammal of origin,

from shrews to whales. This result is in marked contrast to cells *in vivo*, where they are highly constrained by macroscopic transport networks that force their energy production rates to decrease as $M^{-1/4}$. Once the network constraint is removed, as in a culture, energy rates of cells from all mammals converge to the same predicted value as shown in Fig. 2.

A critical test of the generality of our theoretical model will be to extend it explicitly to include unicellular organisms and subcellular structures, to characterize the pathways of intracellular transport, and to identify the cellular organelles and molecular structures involved. Our results suggest that all biological transport systems that exhibit quarter-power allometric scaling must have the same three basic properties of the general model: a space-filling branching network extends throughout the whole organism, the final branch of the network is a size-invariant unit, and the energy required to transport materials is minimized. Finally, the molecular respiratory enzymes must represent the indivisible “lower cutoff” or ultimate terminal unit of the fractal-like transport systems that supply aerobic metabolism. The success of this explanation suggests how nature, via natural selection, has exploited a few very general physical, geometrical, and biological principles to produce the myriad diversity of life.

Appendix: Extrapolation of Metabolic Rate and the Mass of the Smallest Mammal

In arteries, the minimization of energy expenditure requires impedance matching for pulse waves at branch points, thereby leading to area-preserving branching, meaning that the cross-sectional area of a parent branch is equal to the sum of those of the daughters; thus, the ratio of their radii is $n^{-1/2}$, where n , the branching ratio, is the number of daughter branches per parent branch (6). Together with the space-filling constraint, this leads to metabolic rate (the overall volume flow rate) scaling as $M^{3/4}$. In capillaries, on the other hand, radii are so small that significant pulsatile flow cannot be sustained: viscosity dominates and waves are damped heavily, minimization of energy dissipation then leads to Murray’s law where the ratio of radii is $n^{-1/3}$, and the branching is area-increasing such that the flow rate almost ceases. Although the branching changes continuously from one mode to the other, the region of change is relatively narrow, and its location (as measured by the number of branchings from the capillaries) is independent of body mass, M . As the overall size of the organism decreases, the number of area-preserving branchings decreases until a point is reached at which only area-increasing branchings remain; the system is over-

damped and can no longer support pulsatile waves. The value of M at this point defines μ . The dominance of pulsatile flow in the overall network plays a crucial role in deriving the three-quarter power law for B (Eq. 1). As body size decreases, a point is reached at which even major arteries are too constricted to support pulsatile waves; the system becomes so overdamped that waves can no longer propagate, and significant energy is dissipated.

Eq. 4. implies that specific metabolic rate, \bar{B} , the energy required to sustain a unit mass of an organism, changes from a decreasing function of size, $B_0 M^{-1/4}$ when $M > \mu$, to a constant, $B_0 \mu^{-1/4}$, when $M < \mu$. Now the inverse of \bar{B} is a measure of the efficiency of the system, thus this implies that there is a dramatic drop in efficiency when $M < \mu$ because of large energy dissipation from overdamping in the network. This strongly suggests that only mammals with $M > \mu$ could have evolved, thereby providing a fundamental reason for a minimum size for mammals.

This minimum size (μ) can be calculated as follows: for a given mammal, the crossover point from pulsatile to nonpulsatile flow occurs when (6) $r^2/l \approx 8\nu/\rho c_0$, where r is the radius, l is the length of the corresponding branch vessel, ν is the viscosity of blood, ρ is its density, and $c_0 = (Eh/2\rho r)^{1/2} \approx 600 \text{ cm} \cdot \text{sec}^{-1}$ (where E is the modulus of elasticity of the vessel wall and h is its thickness). As the overall size of the mammal decreases, the branching level at which the crossover occurs eventually reaches the aorta. The mass of the mammal in which this occurs defines μ . Using the scaling relations, $r \propto M^{3/8}$ and $l \propto M^{1/4}$, leads straightforwardly to $\mu \approx M(8\nu/\rho c_0^2)^2$, where M is the mass of an arbitrary mammal. Taking $\rho \approx 1 \text{ g} \cdot \text{cm}^{-3}$, $\nu \approx 0.04$ poise, and for a 10-kg mammal, $r \approx 0.75 \text{ cm}$ and $l \approx 20 \text{ cm}$ gives $\mu \approx 3 \text{ g}$, close to the mass of a shrew, which is indeed the smallest mammal. Given the approximations made, the precise value of μ should not be taken too seriously; however, the calculation does show that the model predicts μ to be in the range of 1 g, which, for convenience, is the value used in the text for estimating related quantities. Because most of these estimates depend on $\mu^{1/4}$, the precise value of μ is not critical.

G.B.W. thanks the Mathematics Department at Superl College and the Theoretical Physics Department at Oxford for their hospitality and the Engineering and Physical Sciences Research Council for its support. G.B.W. was supported by Department of Energy Contract ERWE161 and National Science Foundation Grant PHY-9873638, and W.H.W. was supported by National Institutes of Health Grant DK36263 and Department of Energy Grant F629. J.H.B. and G.B.W. also acknowledge the generous support of the Thaw Charitable Trust and a Packard Interdisciplinary Science Grant.

- Kleiber, M. (1932) *Hilgardia* **6**, 315–353.
- Schmidt-Nielsen, K. (1984) *Scaling: Why Is Animal Size so Important?* (Cambridge Univ. Press, Cambridge, U.K.).
- Peters, R. H. (1983) *The Ecological Implications of Body Size* (Cambridge Univ. Press, Cambridge, U.K.).
- Hemmingsen, A. M. (1950) *Rep. Stenographic Mem. Hosp. (Copenhagen)* **4**, 1–58.
- Klas, K. J. (1994) *Plant Allometry: The Scaling of Form and Process* (Univ. of Chicago Press, Chicago).
- West, G. B., Brown, J. H. & Enquist, B. J. (1997) *Science* **276**, 122–126.
- West, G. B., Brown, J. H. & Enquist, B. J. (1999) *Science* **284**, 1677–1679.
- Hochachka, P. W. (1999) *Proc. Natl. Acad. Sci. USA* **96**, 12233–12239.
- Mannella, C. A. (1997) *J. Bioenerg. Biomembr.* **29**, 525–530.
- Yaffe, M. P. (1999) *Science* **283**, 1493–1497.
- Heusner, A. A. (1991) *J. Exp. Biol.* **160**, 25–54.
- Schwerzmann, K., Hoppeler, H., Kayar, S. R. & Weibel, E. R. (1989) *Proc. Natl. Acad. Sci. USA* **86**, 1583–1587.
- Rumsey, W. L., Schlosser, C., Nuutinen, E. M., Robiolo, M. & Wilson, D. F. (1990) *J. Biol. Chem.* **265**, 15392–15399.
- Jansky L. (1961) *Nature (London)* **189**, 921–922.
- Smith, R. E. (1956) *Ann. N.Y. Acad. Sci. USA* **62**, 403–422.
- Villani, G. & Attardi, G. (1997) *Proc. Natl. Acad. Sci. USA* **94**, 1166–1171.
- Hofhaus, G., Johns, D. R., Hurko, O., Attardi, G. & Chomyn, A. (1996) *J. Biol. Chem.* **271**, 13155–13161.
- Guan, M.-X., Fischel-Ghodsian, N. & Attardi, G. (1996) *Hum. Mol. Genet.* **5**, 963–971.
- Dunbar, D. R., Moodie, P. A., Zeviani, M. & Holt, I. J. (1996) *Hum. Mol. Genet.* **5**, 123–129.
- Babcock, G. T. & Wikstrom, M. (1992) *Nature (London)* **356**, 301–309.
- Economos, A. C. (1979) *Gerontology* **26**, 90–98.
- Azbel, M. Y. (1994) *Proc. Natl. Acad. Sci. USA* **91**, 12453–12457.
- Barja, G., Cadenas, S., Rojas, C., Perez-Campo, R. & Lopez-Torres, M. (1994) *Free Radical Res.* **21**, 317–327.
- Guppy, M., Kong, S. E., Niu, X. W., Busfield, S. & Klinken, S. P. (1997) *J. Cell. Physiol.* **170**, 1–7.
- Bereiter-Hahn, J., Munnich, A. & Woiteneck, P. (1998) *Cell Struct. Funct.* **23**, 85–93.
- Yamada, K., Furoushu, S., Sugahara, T., Shirahata, S. & Murakami, H. (1990) *Biotechnol. Bioeng.* **36**, 759–762.
- Bredel-Geissler, A., Karbach, U., Walenta, S., Vollrath, L. & Mueller-Klieser, W. (1992) *J. Cell. Physiol.* **153**, 44–52.
- Yamada, T., Yang, J. J., Ricchiuti, N. V. & Seraydarian, M. W. (1985) *Anal. Biochem.* **145**, 302–307.
- Metzen, E., Wolff, M., Fandry, J. & Jelkmann, W. (1995) *Respir. Physiol.* **100**, 101–106.
- Biaglow, J. E., Varnes, M. E., Jacobson, B. & Suit, H. D. (1984) *Adv. Exp. Med. Biol.* **160**, 323–332.
- Kallinowski, F., Tyler, G., Mueller-Klieser, W. & Vaupel, P. (1989) *J. Cell. Physiol.* **138**, 183–191.
- Gauthier, T., Denis-Pouxviel, C. & Murat, J. C. (1990) *Int. J. Biochem.* **22**, 411–417.
- Hystad, M. E. & Rofstad, E. K. (1994) *Int. J. Cancer* **57**, 532–537.